Conformational disorder in 4-(5,5′-dibromo-2′-chloro-4,4′-bipyridyl-2-yl)-benzaldehyde: role of π–π and halogen interactions

Mohamed Abboud,[a] Amal Kadimi,[b] Victor Mamane[b] and Emmanuel Aubert[a]*

[a]Cristallographie, Résonance Magnétique et Modélisations (CRM2) UMR CNRS–UHP 7036 Institut Jean Barriol, Nancy Université, BP 70239, Boulevard des Aiguillettes, 54506 Vandoeuvre-les-Nancy, France, and [b]Equipe Synthèse Organométallique et Réactivité (SOR), Laboratoire SRSMC, UMR CNRS–UHP 7565 Institut Jean Barriol, Nancy Université, BP 70239, Boulevard des Aiguillettes, 54506 Vandoeuvre-les-Nancy, France

Correspondence e-mail: emmanuel.aubert@crm2.uhp-nancy.fr

The crystal packing of the title compound, $C_{17}H_9Br_2ClN_2O$, is governed by strong π–π stacking, where molecules are tightly bound within infinite (100) planes; these planes interact mainly through non-optimal π–π stacking where arene rings are noticeably displaced from perfect overlap, and also through halogen–halogen interactions. The aldehyde group shows conformational disorder, with a significant population difference between the two conformers; this difference is rationalized by the energetic analysis of the crystal packing using the PIXEL method, which also allows a decomposition of intermolecular interaction energy into Coulombic, polarization, dispersion and repulsion contributions. Using such an analysis, it is found that the main reason for this unequal population of the two conformers in the crystal is two hydrogen bonds that are present only for the major conformer.

Comment

4,4′-Bipyridines are known as good ligands in coordination chemistry and have therefore often been used as building blocks in supramolecular chemistry (Roesky *et al.*, 2003). Recently, a new synthetic method has been developed, which allows the effective formation of halogenated bipyridines (Abboud *et al.*, 2010) that can, in principle, be functionalized by cross-coupling reactions. In a first attempt, the title compound, (I), was prepared by a palladium-catalysed cross-coupling reaction, namely the Suzuki reaction (Miyaura *et al.*, 1995), between 4-formylbenzeneboronic acid, (II), and halogenated 4,4′-bipyridine, (III) (see the reaction scheme in the *Experimental*). The use of two equivalents of boronic acid,

(II), was expected to provide a product arising from the cross-coupling reaction with both C—Br bonds, which are usually more reactive than C—Cl bonds under Suzuki conditions (Miyaura *et al.*, 1995). Moreover, under similar reaction conditions, 5-bromo-2-chloropyridine [the monomeric equivalent of (III)] has been shown to react selectively on the C—Br bond (Belfrekh *et al.*, 2001). However, purification of the reaction mixture afforded compound (I) as the major product in 20% yield, where the coupling occurred at one C—Cl bond. Other minor products coming from the double and triple cross-coupling were also isolated and characterized by NMR and mass spectrometry analyses. Presumably, the steric hindrance around the biaryl connection in compound (III) avoids the palladium approach and insertion in the C—Br bond.

(I)
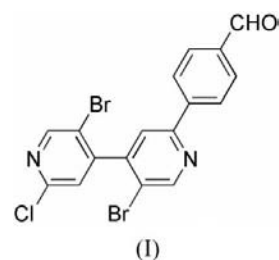
The title compound, (I), crystallizes in the $P\bar{1}$ space group, with one molecule per asymmetric unit. Intramolecular bond distances and angles lie within common values (Allen *et al.*, 1995). The dihedral angle between the pyridine rings is 65.77 (5)°, the intramolecular Br1···Br2 distance being much larger [4.9549 (3) Å] than twice the bromine van der Waals radius (1.85 Å; Bondi, 1964).

The bonded benzaldehyde and pyridine rings are nearly coplanar [dihedral angle = 8.37 (9)°]. The aldehyde group is disordered into two unequally populated orientations coplanar with the arene ring, the occupation factor of the major conformer being 0.740 (5) (Fig. 1).

Intermolecular interactions were analysed through the *OPiX* program package using the PIXEL method (Gavezzotti, 2003*a,b*), which allows a decomposition of intermolecular interaction energies within pairs of molecules into the sum of
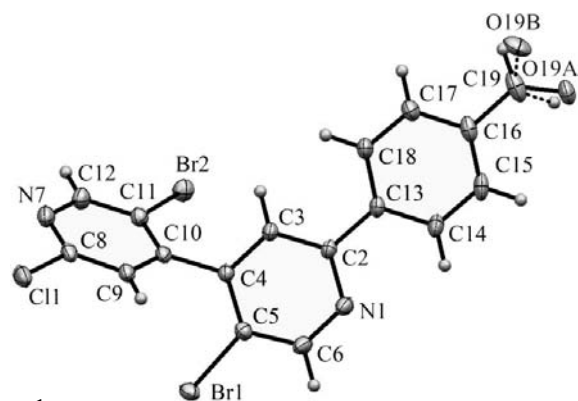
Figure 1
The molecular structure of (I), showing the conformational disorder of the aldehyde group (for clarity, C=O and C—H bonds are drawn as dashed lines for the minor *B* conformer). Atomic displacement ellipsoids are drawn at the 50% probability level.

organic compounds

Coulombic, polarization, dispersion and repulsion contributions. In this PIXEL method, all symmetry-related molecules within 22 Å of a reference molecule were considered; atomic coordinates derived from the X-ray diffraction experiment modelling were used, except for H atoms which were moved to standard average distances, derived from neutron diffraction (Allen *et al.*, 1995). A quantum chemical calculation was then performed on the isolated reference molecule [MP2 level with 6–31G** basis set; *GAUSSIAN03* program package (Frisch *et al.*, 2004)] to obtain the molecular charge density. This latter was then projected on a pixel grid and, together with the atomic nuclei, used to compute the Coulombic contribution to the intermolecular interaction energy. Tabulated atomic polarizabilities (distributed on the previous pixel grid) were used for the evaluation of the polarization and dispersion terms, whereas the repulsion contribution was obtained from the charge-density overlap between the interacting molecules. Owing to the disorder of the aldehyde group into two conformations, this PIXEL energetic analysis was then performed on two hypothetical crystal structures, each of which was built from only one molecular conformation (labelled *A/B* for the major/minor conformations, respectively).

Table 1 reports the intermolecular interaction energies for these two conformations: in both cases the strongest interaction implies a π–π stacking between molecules related by an inversion centre, through their halogenated pyridine rings (Table 2). As shown from the energetic decomposition, this first interaction is characterized by an important Coulombic contribution, completed by an even stronger dispersion term, leading to a net interaction energy almost four times that found for the benzene dimer (Gavezzotti, 2005). Beside the obvious π–π nature of this interaction, shown by a short interplanar distance together with a slippage angle of the aromatic rings of less than 20°, in this particular molecular arrangement two C3—H3$\cdots$Cl1($-x$, $-y$, $-z + 1$) contacts are in favourable geometric orientations (Table 3), with the C—H bond direction pointing to the side of the halogen atom (Desiraju & Steiner, 1999).

Of slightly lower energetic weight, the next two molecular pairs imply two other π–π interactions binding neighbouring molecules around inversion centres (entries 2 and 3 of Table 1). In this case, the stacking involves for each partner the benzaldehyde and the pyridine ring to which it is bonded; in the first of these two molecular pairs, a C9—H19$\cdots$O19A($-x$, $-y$, $-z + 2$) hydrogen bond is also present for conformer *A* but is absent for conformer *B*, the energy difference being about 7.9 kJ mol^{-1} in favour of the major *A* conformer. Remarkably, the presence of this hydrogen bond is associated with a two times larger Coulombic part of the interaction energy. For the second molecular pair no particular differences among conformers are found; in each case, Br2 seems to be docked between H14 and H15 in the molecule at ($-x$, $-y + 1$, $-z + 2$) without establishing any strong interaction (H$\cdots$Br distances are rather long at 3.3–3.4 Å), probably inducing the intramolecular angle between the two pyridine rings through steric interactions. These first three strong π–π

interactions build molecular planes parallel to (100) where molecules are tightly bound (Fig. 2).

The next molecular pair (entry 4, Table 1) is characterized by a kind of π–π stacking between pyridine rings. However the centroids of these two rings are noticeably displaced relative to one another; it appears that this interaction may involve N7—C12—C11—Br2 bonds rather than the entire rings. Contrary to the strongest π–π stacking already reported, this particular interaction has a very small Coulombic contribution but also participates in the cohesion of (100) molecular planes.

Next (entry 5, Table 1) is an interaction which relates two benzaldehyde groups, linking adjacent molecular planes along the [100] direction. In an even more marked fashion than the previous case, the two ring centroids are considerably offset relative to one another (slippage angle = 56.4°); no π-cloud overlapping can be invoked. However, the proximity of the two molecules induces a significant dispersion contribution; in the case of conformer *B*, where the O atom of the aldehyde group is closer to the neighbouring arene ring, an unfavourable Coulombic term arises, probably due to the counterproductive proximity of the electronegative O atom and of the arene π-cloud.

The next intermolecular interaction involves a cyclic CH$\cdots$N dimer (entry 6, Table 1), forming an $R_2^2(6)$ motif; the energy decomposition shows a predominantly dispersive character with a reduced Coulombic part, linked to the fact that the interatomic H$\cdots$N distances are large (Table 3). In comparison, the next molecular pairs (entries 7 and 8, Table 1) which display cyclic C12—H12$\cdots$O19A(x, y, $z - 1$) and C15—H15$\cdots$N7(x, y, $z + 1$) hydrogen bonds [$R_2^2(8)$ motif] for conformer *A*, have a stronger Coulombic energy. In conformer *B*, where the aldehyde is rotated by 180°, only the C15—H15$\cdots$N7(x, y, $z + 1$) hydrogen bond is present to assist cohesion in the (100) plane through a $C(11)$ motif; this induces a decrease in the stabilizion energy of about 4.4 kJ mol^{-1} in comparison with conformer *A*.

The last molecular pairs with interaction energies below or around -10 kJ mol^{-1} (entries 9, 10 and 11, Table 1) imply homogeneous and heterogeneous halogen–halogen interactions participating in the cohesion between (100) planes.
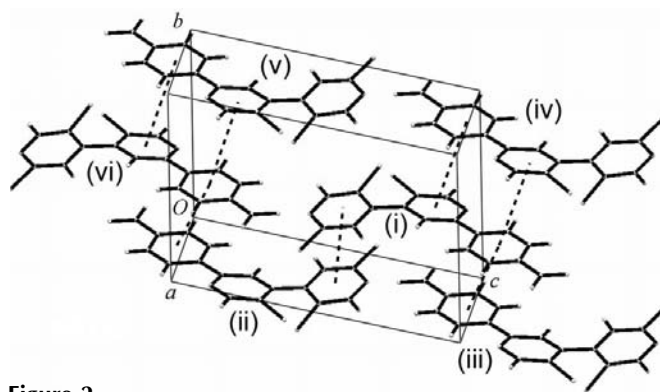
Figure 2
Packing diagram showing the (100) plane; the first three strongest π–π stacking interactions are shown as dashed lines. [Symmetry codes: (i) x, y, z; (ii) $-x$, $-y$, $1 - z$; (iii) $-x$, $-y$, $2 - z$; (iv) $-x$, $1 - y$, $2 - z$; (v) $-x$, $1 - y$, $1 - z$; (vi) x, y, $-1 + z$.]

The Br1$\cdots$Br2($x + 1, y, z$) interaction is of type II (Reddy *et al.*, 2006), with the C11—Br2 bond pointing towards the side of Br1($x - 1, y, z$) (Table 4). In such a geometric arrangement, the positive σ charge hole beyond Br2 faces the negative charge crown around Br1 in the molecule at ($x - 1, y, z$). Despite this electrostatic interaction scheme, it can be seen from Table 1 that this molecular pair is still dominated by dispersion; this is because the energy decomposition applies to the whole molecule which displays strong electron delocalization and thus is prone to significant dispersion. The dispersive and repulsive (respectively, Coulombic and polarization) contributions are in this case even more (respectively, less) pronounced than in the previous molecular pair, implying hydrogen bonds. For both conformers a heterogeneous halogen–halogen interaction is also present, with the C5—Br1 bond pointing towards the Cl1($-x + 1, -y + 1, -z + 1$) negative crown, thus also of type II. Because this particular stacking induces two such Br$\cdots$Cl halogen bonds, the energy gained per bond is noticeably small (-4.6 kJ mol^{-1}) compared to the stabilization energy for the previous Br$\cdots$Br contacts (-10.6 kJ mol^{-1}). However, this heterogeneous halogen bond could be stronger in the crystal than was shown in this energetic analysis between pairs of molecules. This C5—Br1$\cdots$Cl1($-x + 1, -y + 1, -z + 1$) interaction may be strengthened by the polarization of Br1 due to the presence of the C11Br2$\cdots$Br1 interaction; indeed, co-operativity of halogen bonds has been shown to exist in model clusters of diatomic interhalogen molecules (Alkorta *et al.*, 2009).

Most of the remaining weakly bound molecular pairs show no clear characteristics and include distant molecules without direct intermolecular interaction (*i.e.* involving the second interaction shell around the reference molecule). An exception is an interatomic contact with a distance less than the sum of the van der Waals radii for conformer *A*, between Cl1 and O19*A*($x + 1, y, z - 1$) (Table 5). This can be rationalized from an electrostatic point of view since the C8—Cl1 bond direction is towards the negatively charged O atom. However, this contact is characterized by a relatively significant repulsion contribution, which makes the *B* conformer more stable in this particular situation, although the invoked energies are extremely weak.

In summary, it can be seen from the above analysis that conformer *A* leads to more stabilizing intermolecular interactions than conformer *B*, the energy difference being 13.2 kJ mol^{-1}; this is in agreement with the fact that, in the investigated sample, there are significantly more molecules with the *A* conformation of the aldehyde group.

Experimental

To a degassed toluene solution (6 ml) containing Pd(PPh₃)₄ (87 mg, 0.075 mmol) and (III) (575 mg, 1.5 mmol) were successively added degassed solutions of (II) (450 mg, 3 mmol) in methanol (3 ml) and Na₂CO₃ (636 mg, 6 mmol) in water (3 ml). After heating for 15 h at 373 K, the reaction mixture was cooled to room temperature, extracted with ethyl acetate and dried over MgSO₄. After concentration, the residue was purified by chromatography on silica gel (hexanes/ethyl acetate, 9/1 *v/v*) to give compound (I) as a yellow powder (yield 136 mg, 20%). Crystals of (I) were obtained by slow evaporation of a chloroform solution at room temperature and in air (m.p. 443–444 K).
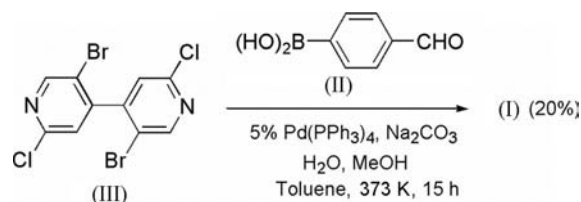
^{1}H NMR (CDCl₃, 200 MHz): δ 10.08 (*s*, 1H), 8.95 (*s*, 1H), 8.67 (*s*, 1H), 8.18 (*d*, *J* = 6.6 Hz, 2H), 7.99 (*d*, *J* = 6.6 Hz, 2H), 7.65 (*s*, 1H), 7.29 (*s*, 1H); ^{13}C NMR (CDCl₃, 50 MHz): δ 191.7, 155.1, 152.7, 152.2, 150.7, 149.4, 146.6, 142.9, 137.1, 130.4, 127.5, 125.3, 121.7, 119.9, 119.3; MS (70 eV), *m/z* (%): 452 (100%, [*M*]$^+$), 423 (25%, [*M* − CHO]$^+$), 228 (20%, [*M* − 2Br − CHO]); HRMS *m/z* calculated for C₁₇H₉Br₂Cl-N₂O: 452.8822, found: 452.8827.

Crystal data

C₁₇H₉Br₂ClN₂O	$\gamma = 104.401\ (2)°$
$M_r = 452.53$	$V = 787.52\ (3)$ Å^3
Triclinic, $P\bar{1}$	$Z = 2$
$a = 7.5759\ (2)$ Å	Mo $K\alpha$ radiation
$b = 8.4629\ (2)$ Å	$\mu = 5.32$ mm^{-1}
$c = 13.1534\ (2)$ Å	$T = 110$ K
$\alpha = 103.082\ (2)°$	$0.22 \times 0.15 \times 0.07$ mm
$\beta = 94.473\ (2)°$	

Data collection

Oxford Diffraction SuperNova Dual diffractometer with an Atlas detector	derived by Clark & Reid (1995)]
	$T_{min} = 0.444$, $T_{max} = 0.758$
	35546 measured reflections
Absorption correction: analytical [*CrysAlis Pro* (Oxford Diffraction, 2009), based on expressions	5351 independent reflections
	4767 reflections with $I > 2\sigma(I)$
	$R_{int} = 0.028$

Table 1
Intermolecular interaction energies within pairs of molecules [the reference molecule is (x, y, z)].

d is the distance between molecular mass centres (Å); Coul., Pol., Disp. and Rep. are, respectively, Coulombic, polarization, dispersion and repulsion contributions to the total interaction energy for conformer *A* (Tot. *A*). For each molecular pair, the corresponding interaction energies obtained for the *B* conformer are also reported (Tot. *B*). Energies are given in kJ mol^{-1}.

No.	d	Symmetry	Coul.	Pol.	Disp.	Rep.	Tot. *A*	Tot. *B*
1	7.358	$-x, -y, 1 - z$	−21	−8.1	−53.3	36.3	−46.2	−45.9
2	9.136	$-x, -y, 2 - z$	−23.2	−8.6	−64.5	56.8	−39.5	−31.6
3	6.785	$-x, 1 - y, 2 - z$	−12	−4.1	−66.9	43.6	−39.5	−40.1
4	8.191	$-x, 1 - y, 1 - z$	−4	−1.3	−28.3	13.3	−20.3	−20.6
5	12.021	$-1 - x, -y, 2 - z$	−7.7	−2.6	−22.7	15	−18	−13.7
6	8.239	$1 - x, 1 - y, 2 - z$	−6	−2.1	−20.3	12	−16.4	−16.3
7	13.153	$x, y, -1 + z$	−8.3	−3.7	−13.3	11.9	−13.5	−9.1
8	13.153	$x, y, 1 + z$	−8.3	−3.7	−13.3	11.9	−13.5	−9.1
9	7.576	$-1 + x, y, z$	−5.7	−2.2	−19.2	16.5	−10.6	−11.4
10	7.576	$1 + x, y, z$	−5.7	−2.2	−19.2	16.5	−10.6	−11.4
11	10.222	$1 - x, 1 - y, 1 - z$	−9.4	−3.8	−18.5	22.4	−9.2	−9
12	9.855	$-1 + x, -1 + y, z$	0.3	−2.8	−14	9.7	−6.9	−8.3
13	9.855	$1 + x, 1 + y, z$	0.3	−2.8	−14	9.7	−6.9	−8.3
14	11.11	$1 - x, -y, 1 - z$	−0.6	−0.3	−6.1	1.7	−5.3	−5.4
15	8.463	$x, -1 + y, z$	0.6	−0.1	−2.3	0	−1.9	−2.2
16	8.463	$x, 1 + y, z$	0.6	−0.1	−2.3	0	−1.9	−2.2
17	15.683	$-1 + x, y, 1 + z$	−3.4	−1.5	−5.2	8.6	−1.5	−2.7
18	15.683	$1 + x, y, -1 + z$	−3.4	−1.5	−5.2	8.6	−1.5	−2.7

organic compounds

Refinement

$R[F^2 > 2\sigma(F^2)] = 0.028$	218 parameters
$wR(F^2) = 0.073$	H-atom parameters constrained
$S = 1.07$	$\Delta\rho_{max} = 2.08$ e Å^{-3}
5351 reflections	$\Delta\rho_{min} = -1.25$ e Å^{-3}

Table 2
π–π interactions.

$Cg1$, $Cg2$ and $Cg3$ are the centroids of the N1/C2–C6, N7/C8–C12 and C13–C18 rings, respectively. CCD is the distance between ring centroids, SA is the angle subtended by the intercentroid vector to the plane normal (*i.e.* slippage angle), IPD is the distance from one plane to the neighbouring centroid (mean interplanar distance).

Group 1/Group 2	CCD (Å)	SA (°)	IPD (Å)
$Cg2/Cg2^{i}$	3.708 (2)	18.1	3.5240 (8)
$Cg3/Cg3^{ii}$	3.537 (2)	19.9	3.3255 (9)
$Cg1/Cg3^{iii}$	4.076 (1)	29.9	3.2023 (7)
$Cg3/Cg1^{iii}$	4.076 (1)	38.2	3.5340 (8)
$Cg2/Cg2^{iv}$	5.104 (2)	43.8	3.6865 (8)

Symmetry codes: (i) $-x, -y, 1-z$; (ii) $-x, -y, 2-z$; (iii) $-x, 1-y, 2-z$; (iv) $-x, 1-y, 1-z$.

Table 3
Hydrogen-bond geometry (Å,°).

D—H$\cdots A$	D—H	H$\cdots A$	$D\cdots A$	D—H$\cdots A$
C9—H9$\cdots$O19A^{i}	0.95	2.62	3.269 (3)	126
C12—H12$\cdots$O19A^{ii}	0.95	2.66	3.244 (2)	120
C15—H15$\cdots$N7^{iii}	0.95	2.72	3.530 (3)	144
C6—H6$\cdots$N1^{iv}	0.95	2.82	3.470 (3)	126
C3—H3$\cdots$Cl1^{v}	0.95	2.95	3.870 (1)	162

Symmetry codes: (i) $-x, -y, 2-z$; (ii) $x, y, z-1$; (iii) $x, y, 1+z$; (iv) $1-x, 1-y, 2-z$; (v) $-x, -y, 1-z$.

H atoms were located from difference Fourier maps. The final structure was constructed using riding models for C—H bonds, with interatomic distances fixed at 0.95 Å and U_{iso}(H) values fixed at $1.2U_{eq}$(C) for all H atoms.

Data collection: *CrysAlis Pro* (Oxford Diffraction, 2009); cell refinement: *CrysAlis Pro*; data reduction: *CrysAlis Pro*; program(s) used to solve structure: *SIR2004* (Burla *et al.*, 2005)'; program(s) used to refine structure: *SHELXL97* (Sheldrick, 2008); molecular graphics: *Mercury* (Macrae *et al.*, 2008); software used to prepare material for publication: *PLATON* (Spek, 2009).

Table 4
C—$X\cdots X'$—C' interactions (Å, °) where X/X' = Br/Cl.

C—$X\cdots X'$—C'	C—X	X'—C'	$X\cdots X'$	C—$X\cdots X'$	$X\cdots X'$—C'
C5—Br1$\cdots$(Br2—C11)^{i}	1.889 (2)	1.886 (2)	3.5473 (3)	108.83 (5)	174.79 (5)
C5—Br1$\cdots$(Cl1—C8)^{ii}	1.889 (2)	1.746 (2)	3.4730 (5)	162.92 (5)	101.62 (6)

Symmetry codes: (i) $1+x, y, z$; (ii) $1-x, 1-y, 1-z$.

Table 5
C—Cl$\cdots$O=C' interaction (Å, °).

C—Cl$\cdots$O=C'	C—Cl	O=C	Cl$\cdots$O	C—Cl$\cdots$O	Cl$\cdots$O=C
C8—Cl1$\cdots$(O19A=C19$A)^{i}$	1.889 (2)	1.170 (3)	3.033 (2)	169.16 (7)	132.6 (2)

Symmetry code: (i) $1+x, y, -1+z$.

Professors A. Gavezzotti, C. Lecomte and E. Espinosa for fruitful discussions.

Supplementary data for this paper are available from the IUCr electronic archives (Reference: KU3026). Services for accessing these data are described at the back of the journal.

References

Abboud, M., Mamane, V., Aubert, E., Lecomte, C. & Fort, Y. (2010). *J. Org. Chem.* **75**, 3224–3231.
Alkorta, I., Blanco, F. & Elguero, J. (2009). *Struct. Chem.* **20**, 63–71.
Allen, F. H., Kennard, O., Watson, D. G., Brammer, L., Orpen, A. G. & Taylor, R. (1995). *International Tables for Crystallography*, Vol. C, Section 9.5, pp. 685–706. Dordrecht: Kluwer Academic Publishers.
Belfrekh, N., Dietrich-Buchecker, C. & Sauvage, J.-P. (2001). *Tetrahedron Lett.* **42**, 2779–2781.
Bondi, A. (1964). *J. Phys. Chem.* **68**, 441–451.
Burla, M. C., Caliandro, R., Camalli, M., Carrozzini, B., Cascarano, G. L., De Caro, L., Giacovazzo, C., Polidori, G. & Spagna, R. (2005). *J. Appl. Cryst.* **38**, 381–388.
Clark, R. C. & Reid, J. S. (1995). *Acta Cryst.* A**51**, 887–897.
Desiraju, G. R. & Steiner, T. (1999). *The Weak Hydrogen Bond in Structural Chemistry and Biology*, 1st ed. New York: Oxford University Press Inc.
Frisch, M. J., *et al.* (2004). *GAUSSIAN03*. Revision B.05. Gaussian Inc., Wallingford, Connecticut, USA.
Gavezzotti, A. (2003*a*). *J. Phys. Chem. B*, **107**, 2344–2353.
Gavezzotti, A. (2003*b*). *OPiX*. University of Milano, Italy.
Gavezzotti, A. (2005). *J. Chem. Theory Comput.* **1**, 834–840.
Macrae, C. F., Bruno, I. J., Chisholm, J. A., Edgington, P. R., McCabe, P., Pidcock, E., Rodriguez-Monge, L., Taylor, R., van de Streek, J. & Wood, P. A. (2008). *J. Appl. Cryst.* **41**, 466–470.
Miyaura, N. & Suzuki, A. (1995). *Chem. Rev.* **95**, 2457–2483.
Oxford Diffraction (2009). *CrysAlis Pro*. Version 1.171.33.41. Oxford Diffraction Ltd, Yarnton, Oxfordshire, England.
Reddy, C. M., Kirchner, M. T., Gundakaram, R. C., Padmanabhan, K. A. & Desiraju, G. R. (2006). *Chem. Eur. J.* **12**, 2222–2234.
Roesky, H. W. & Andruh, M. (2003). *Coord. Chem. Rev.* **236**, 91–119.
Sheldrick, G. M. (2008). *Acta Cryst.* A**64**, 112–122.
Spek, A. L. (2009). *Acta Cryst.* D**65**, 148–155.